Electronic Supplementary Information

Nuclear quantum effects in direct ionization processes of pure helium clusters: path-integral and ring-polymer molecular dynamics simulations on the diatomics-in-molecule potential energy surfaces[†]

Kento Suzuki, Takaaki Miyazaki, Toshiyuki Takayanagi[*]
Department of Chemistry, Saitama University, Shimo-Okubo 255, Sakura-ku, Saitama City,
Saitama 338-8570, JAPAN

Motoyuki Shiga
Center for Computational Science and E-Systems, Japan Atomic Energy Agency, 148-4,
Kashiwanoha, Campus, 178-4 Wakashiba, Kashiwa, Chiba 277-0871, Japan

Summary of Electronic Supplementary Information

Table S1 summarizes the SAC-CI and DIM results used in Fig. 1 of the main text. Table S2 summarizes the Cartesian coordinates used in the SAC-CI calculations.

Fig. S1 compares the ionization spectra calculated with the SAC-CI/aug-cc-pVQZ level to the spectra calculated with the SAC-CI/6-31+G(3*df*) level. The same cluster structures in Table S2 were used.

Fig. S2 displays time evolution of the RPMD trajectory for the He_{100}^+ cluster when the initial ionization state is assumed to the 79-th adiabatic excited state. The corresponding adiabatic populations and atomic charges are presented in Fig. S3 as a function of the simulation time.

Fig. S4 shows time evolution of the RPMD trajectory for the He_{200}^+ cluster when the initial ionization state is assumed to the 151-st adiabatic excited state. Notice that the initial positive charge is distributed among several He atoms in this case. The corresponding adiabatic populations and atomic charges are presented in Fig. S5 as a function of the simulation time.

Fig. S6 displays time evolution of the RPMD trajectory for the He_{200}^+ cluster when the initial ionization state is assumed to the adiabatic ground state. The corresponding adiabatic populations and atomic charges are presented in Fig. S7 as a function of the simulation time.

Fig. S8 displays time evolution of the RPMD trajectory for the He_{300}^+ cluster when the initial ionization state is assumed to the adiabatic ground state. The corresponding adiabatic populations and atomic charges are presented in Fig. S9 as a function of the simulation time.

Fig. S10 displays time evolution of the RPMD trajectory for the He_{300}^+ cluster when the initial ionization state is assumed to the adiabatic ground state (a different initial structure from Fig. S8 is used). The corresponding adiabatic populations and atomic charges are presented in Fig. S11 as a function of the simulation time.

Table S1

Numerical data used in Fig. 1 of the main text. The ionization energy levels and the corresponding intensities obtained from the ab initio SAC-CI/aug-cc-pVQZ level calculations and the DIM energy levels are summarized.

	SAC-CI/aug-cc-pVQZ		DIM
State	Energy (eV)	Intensity (Relative Intensity)	Energy (eV)
He_4^+			
1	24.408	0.96956 (0.9991)	24.464
2	24.412	0.96953 (0.9990)	24.464
3	24.435	0.96954 (0.9990)	24.464
4	24.686	0.97048 (1.0000)	24.662
He_5^+			
1	24.394	0.96995 (0.9989)	24.420
2	24.426	0.97015 (0.9991)	24.440
3	24.427	0.97016 (0.9991)	24.440
4	24.531	0.96947 (0.9984)	24.511
5	24.730	0.97101 (1.0000)	24.677
He_6^+			
1	24.331	0.97118 (0.9991)	24.394
2	24.369	0.97129 (0.9992)	24.411
3	24.422	0.97023 (0.9981)	24.417
4	24.444	0.97186 (0.9998)	24.474
5	24.525	0.97208 (1.0000)	24.534
6	24.709	0.97204 (1.0000)	24.688

Table S2

Cartesian coordinates (in unit of Å) for the He_n^+ (n = 4, 5 and 6) clusters used in the SAC-CI calculations

Cluster	X	Y	Z
He_4^+			
He	0.48024	−0.23315	1.22264
He	−1.59088	−1.30019	−0.61956
He	0.51119	0.52891	−1.64793
He	−1.61773	1.57049	0.14224
He_5^+			
He	0.82998	0.25021	0.32845
He	−1.63477	−1.36378	−0.07445
He	−0.91194	0.75659	−2.01709
He	−0.85303	−0.49886	2.65196
He	−1.84269	1.50011	0.69830
He_6^+			
He	0.24333	−0.85590	0.41683
He	−2.47858	−1.35901	−0.64824
He	−0.81788	0.83281	−1.76761
He	0.03135	0.48342	3.04569
He	−1.96488	−1.57035	2.26336
He	−1.96404	1.08755	0.94735

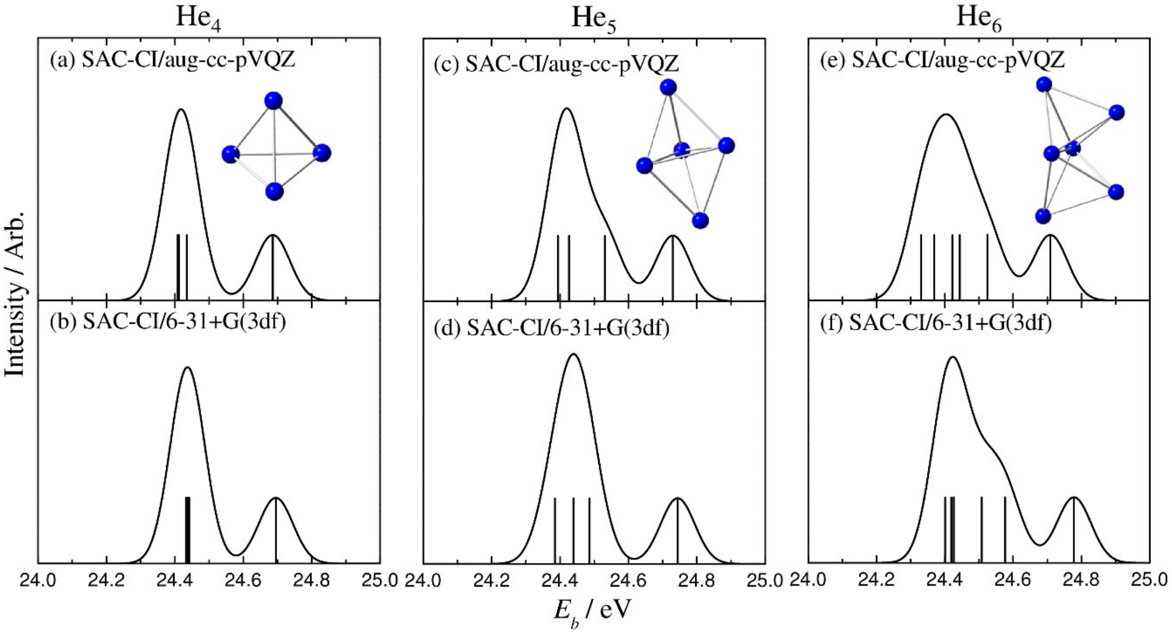

Fig. S1

Comparison of the ionization spectra calculated with the SAC-CI/aug-cc-pVQZ level to the spectra calculated with the SAC-CI/6-31+G(3*df*) level. The same He_n^+ (n = 4–6) cluster structures in Table S2 were used. The discrete ionization energy levels are convoluted using the Gaussian function with 120 meV width.

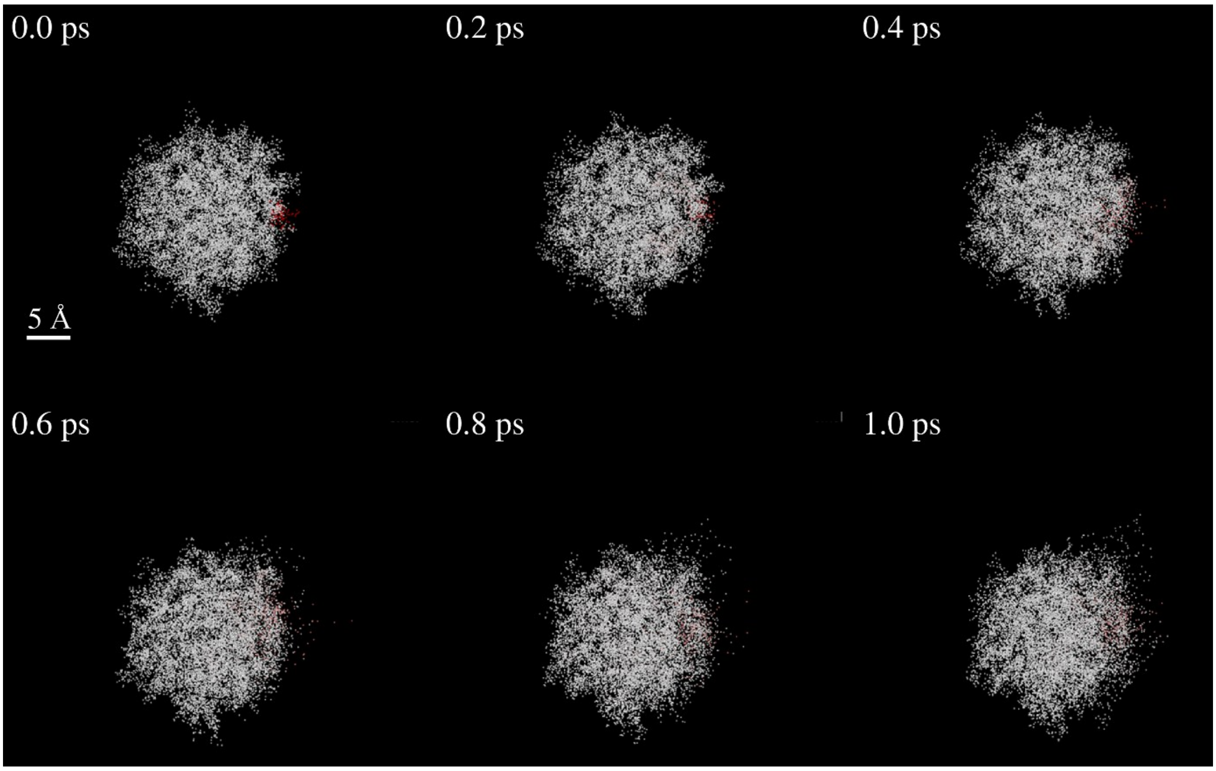

Fig. S2

Snapshots of the nonadiabatic RPMD trajectory showing dynamics evolution of the He_{100}^+ cluster when the initial ionization state is assumed to the adiabatic 79-th excited state, for which the initial charged He atom is mainly located around the surface of the cluster. All ring-polymer beads are shown with the positively charged He atoms being shown in red color. The time interval of the snapshots is chosen to be 0.2 ps.

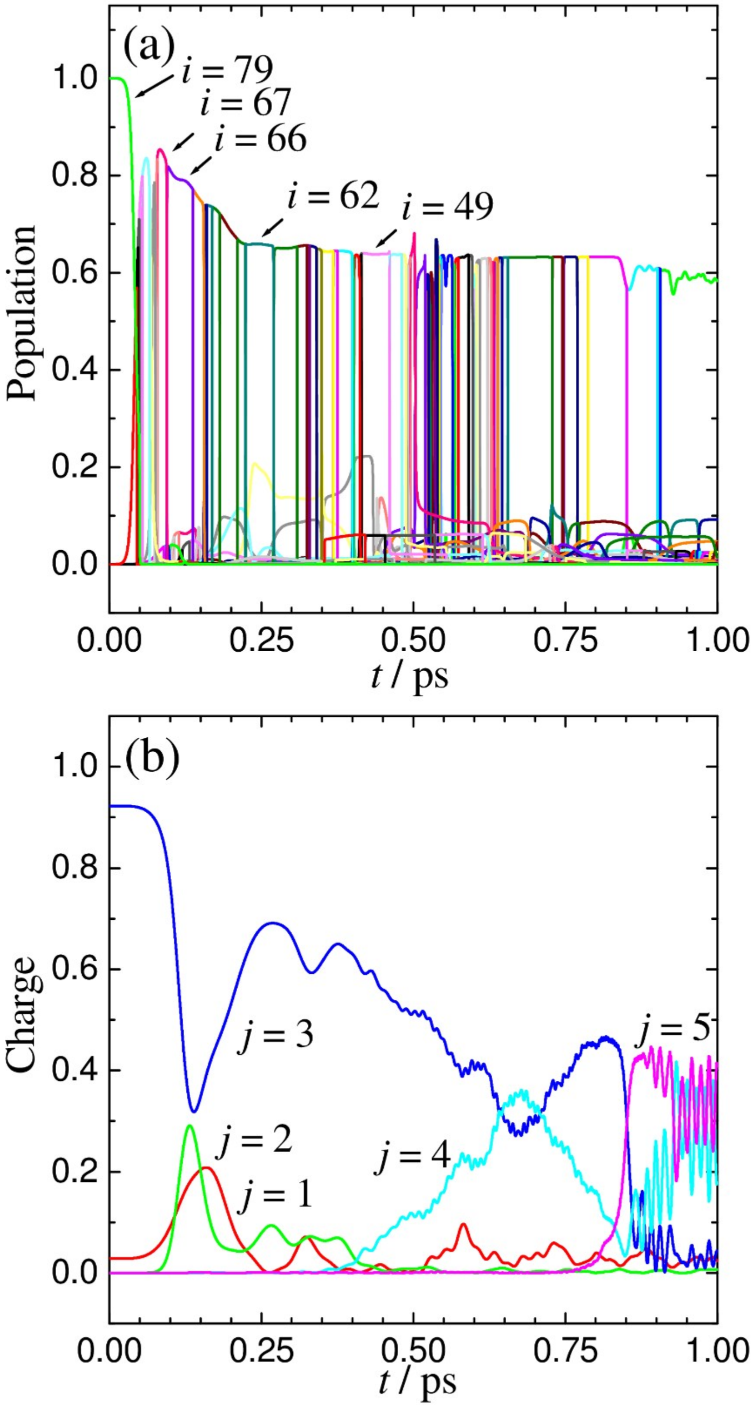

Fig. S3

Selected adiabatic populations (a) and atomic charges (b) are plotted as a function of the simulation time for the representative RPMD trajectory presented in Fig. S2.

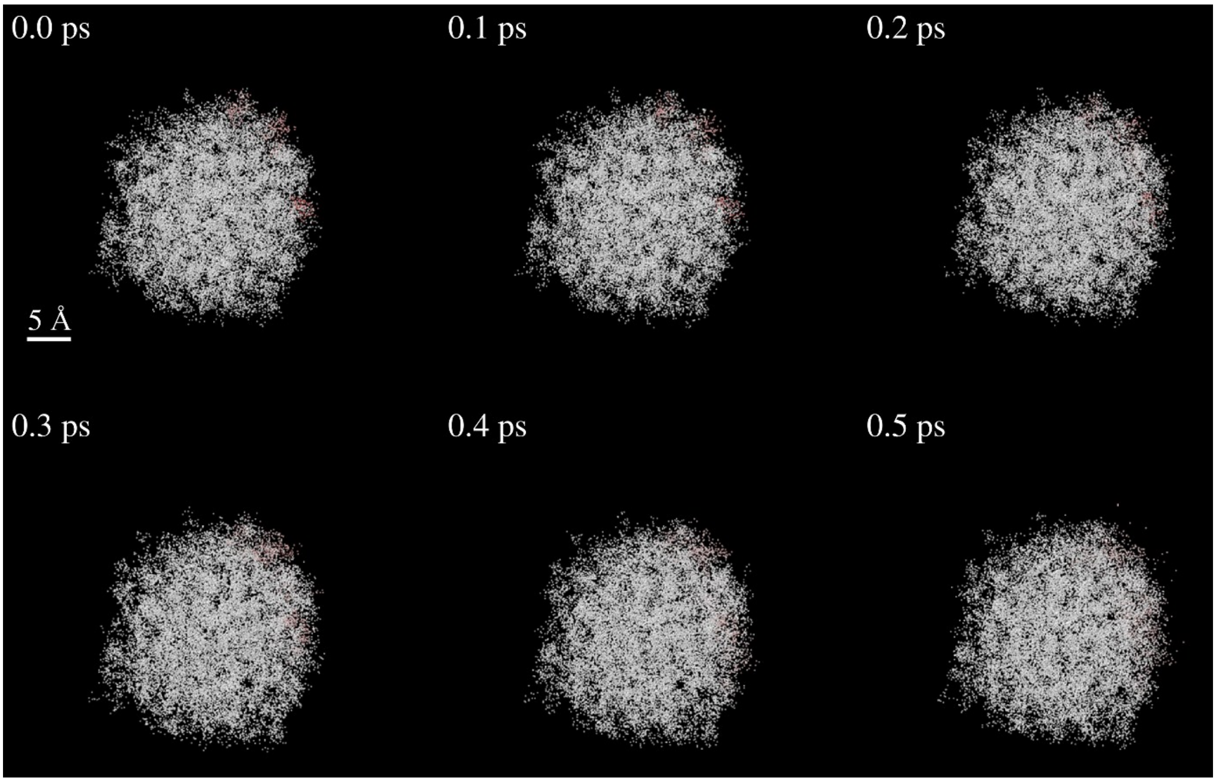

Fig. S4

Snapshots of the nonadiabatic RPMD trajectory showing dynamics evolution of the He_{200}^{+} cluster when the initial ionization state is assumed to the adiabatic 151-st excited state, for which the initial charge is distributed two He atoms, which are mainly located around the surface region of the cluster. All ring-polymer beads are shown with the positively charged He atoms being shown in red color. The time interval of the snapshots is chosen to be 0.1 ps.

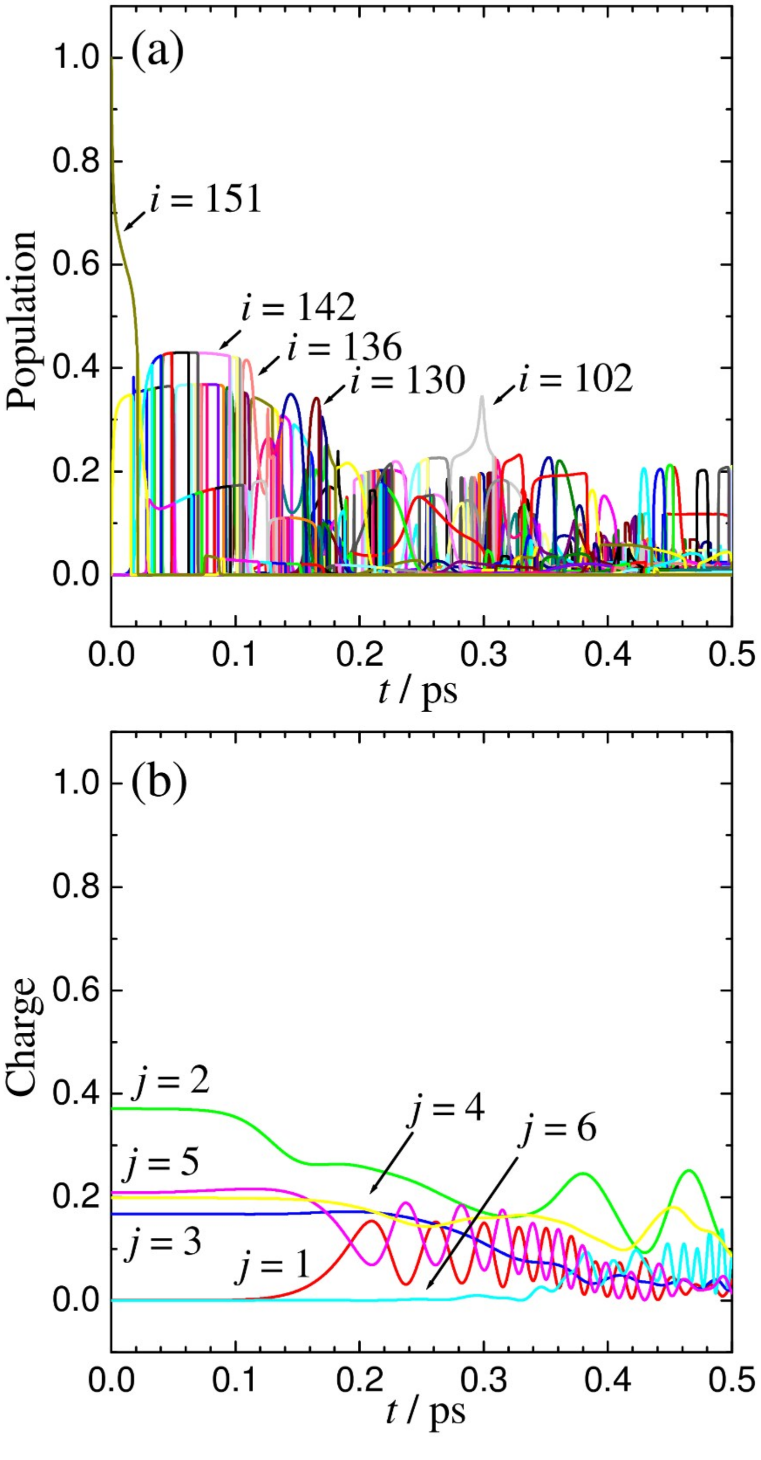

Fig. S5

Selected adiabatic populations (a) and atomic charges (b) are plotted as a function of the simulation time for the representative RPMD trajectory presented in Fig. S4.

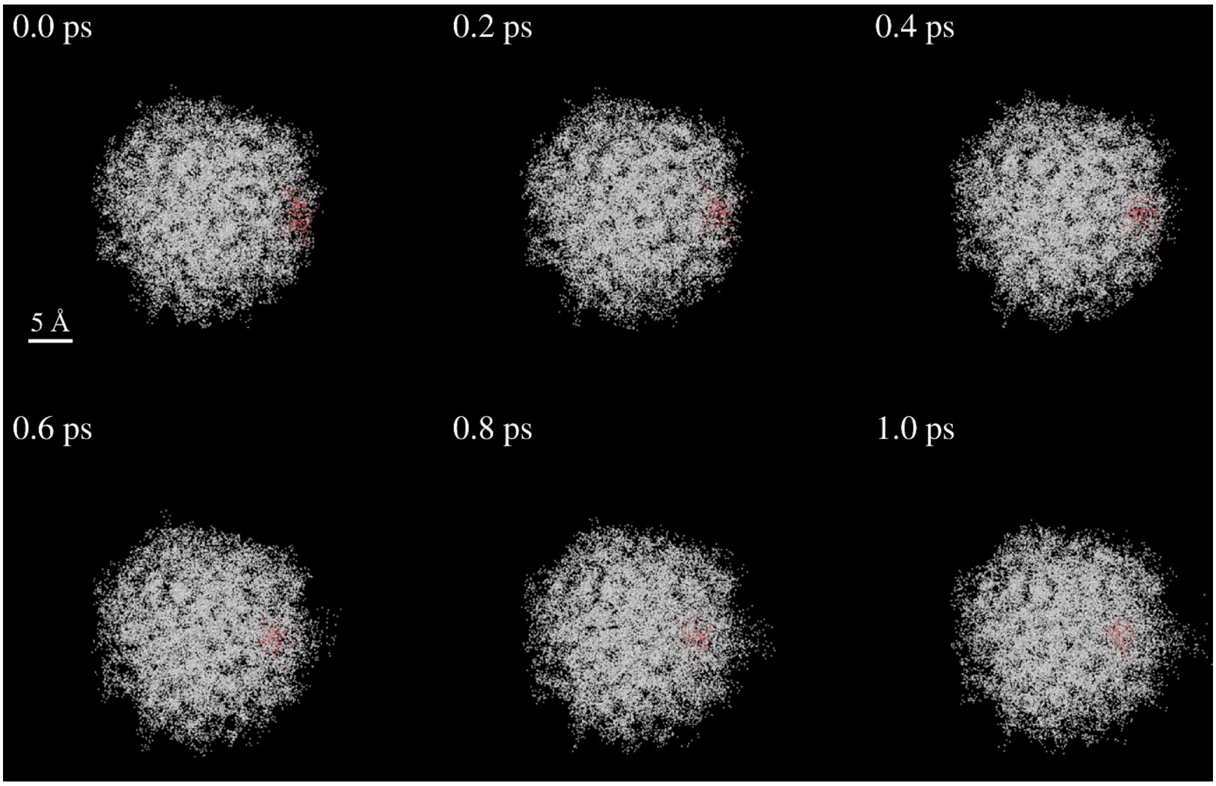

Fig. S6

Snapshots of the nonadiabatic RPMD trajectory showing dynamics evolution of the $He_{200}{}^{+}$ cluster when the initial ionization state is assumed to the adiabatic ground state, for which the initial charge is distributed two He atoms, which are mainly located around the surface region of the cluster. All ring-polymer beads are shown with the positively charged He atoms being shown in red color. The time interval of the snapshots is chosen to be 0.2 ps.

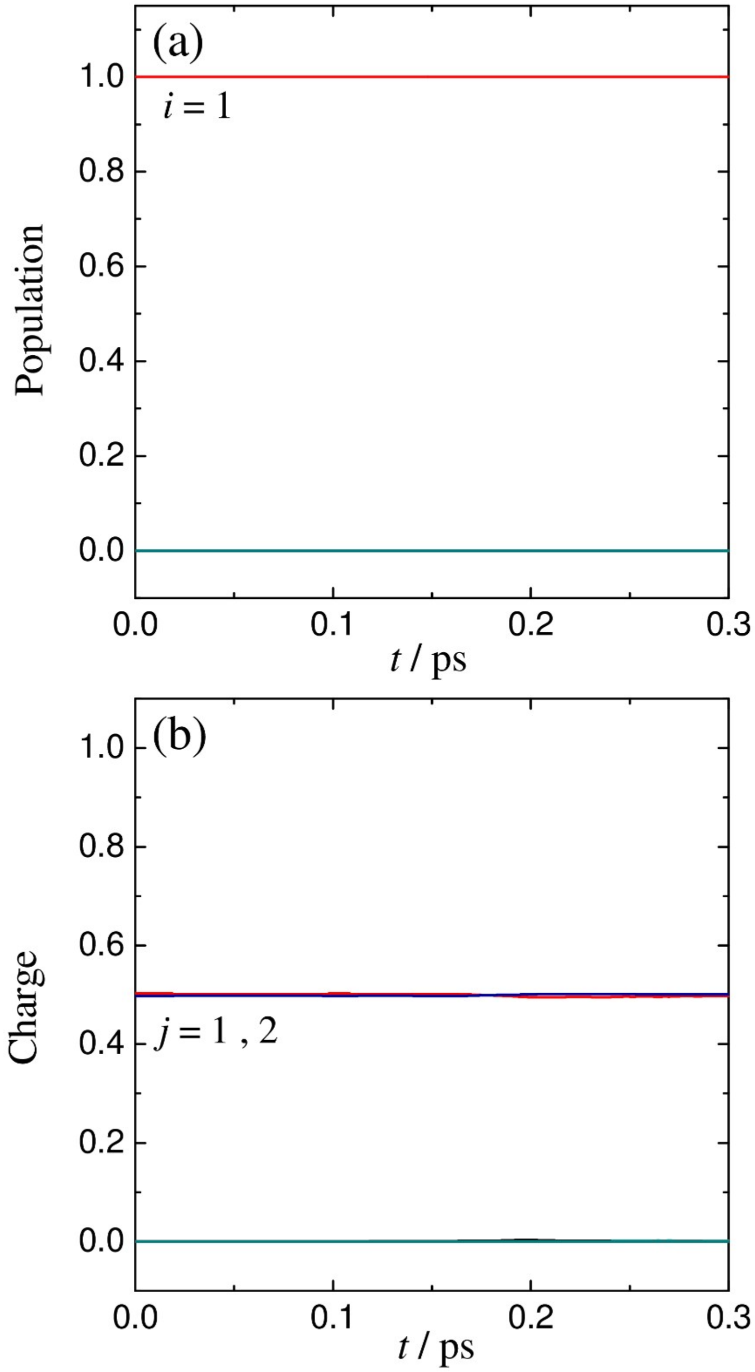

Fig. S7

Selected adiabatic populations (a) and atomic charges (b) are plotted as a function of the simulation time for the representative RPMD trajectory presented in Fig. S6.

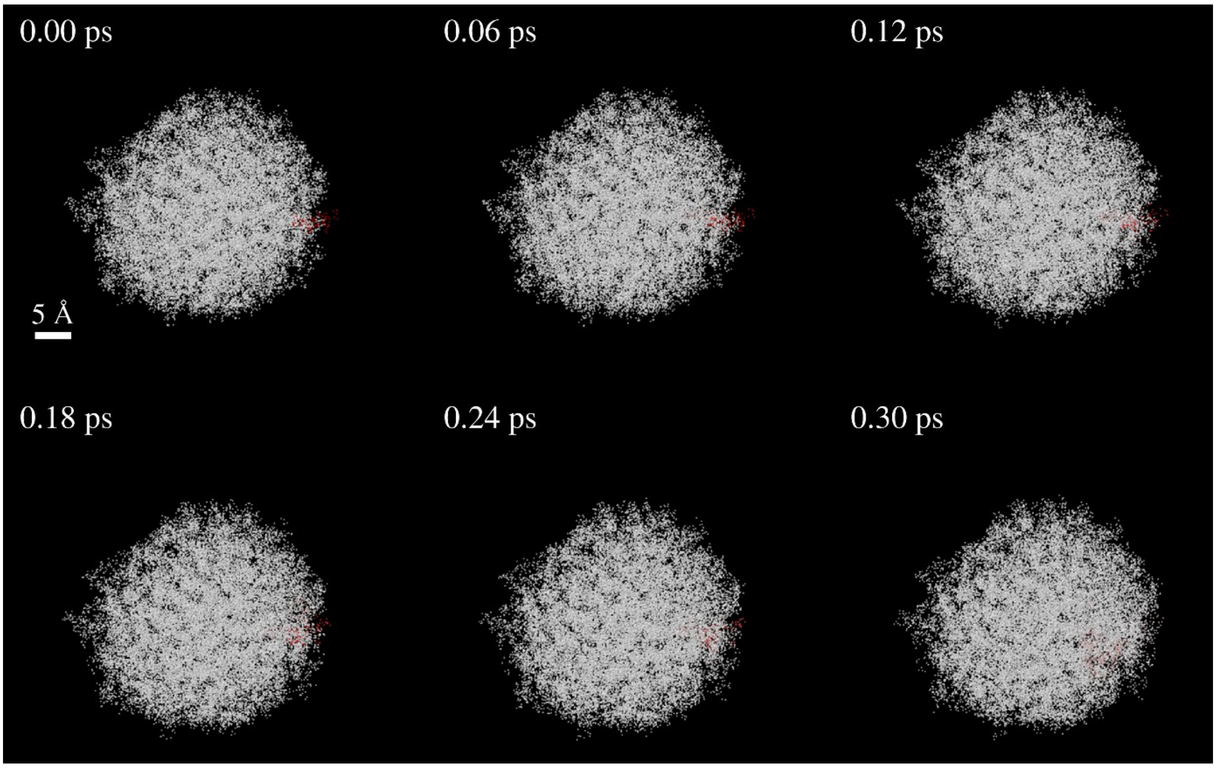

Fig. S8

Snapshots of the nonadiabatic RPMD trajectory showing dynamics evolution of the He_{300}^+ cluster when the initial ionization state is assumed to the adiabatic ground state, for which the initial charged He atom is mainly located around the surface of the cluster. All ring-polymer beads are shown with the positively charged He atoms being shown in red color. The time interval of the snapshots is chosen to be 0.06 ps.

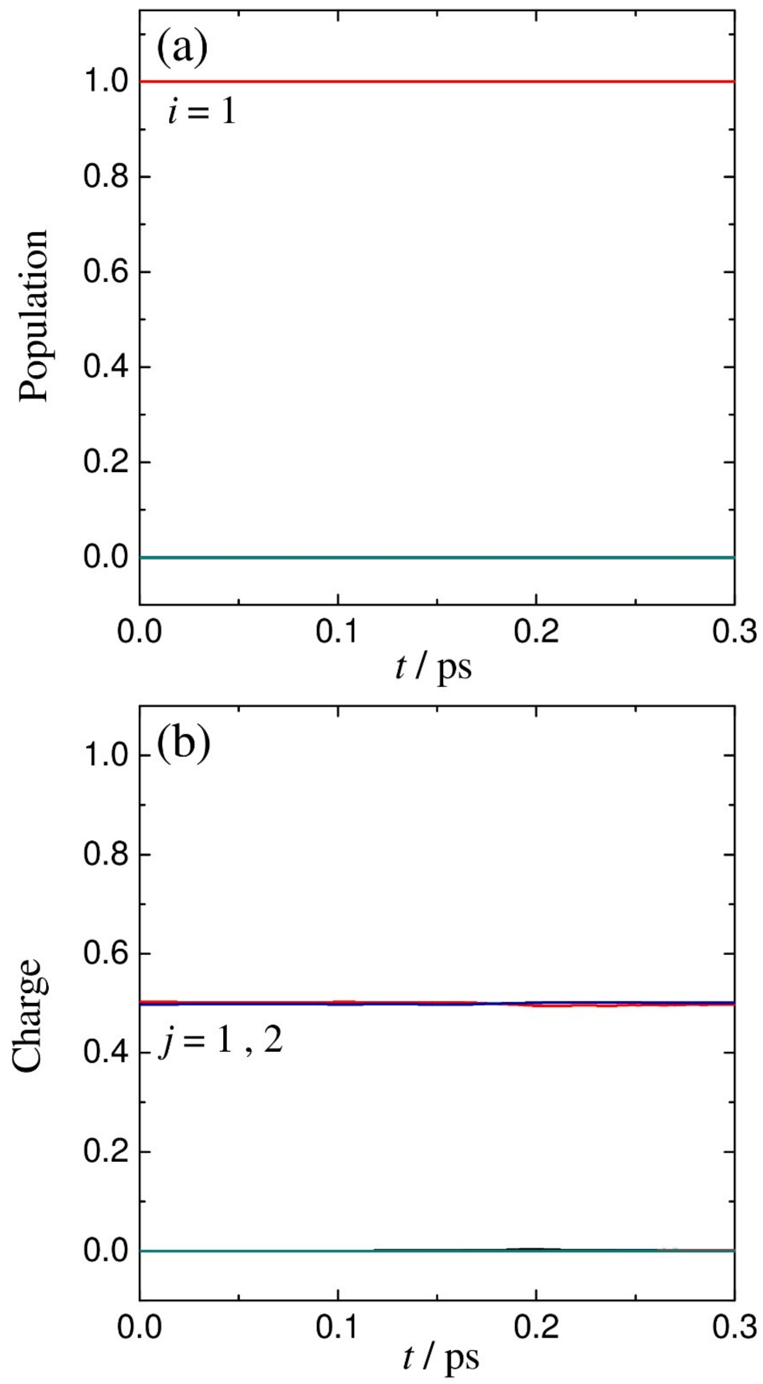

Fig. S9

Selected adiabatic populations (a) and atomic charges (b) are plotted as a function of the simulation time for the representative RPMD trajectory presented in Fig. S8.

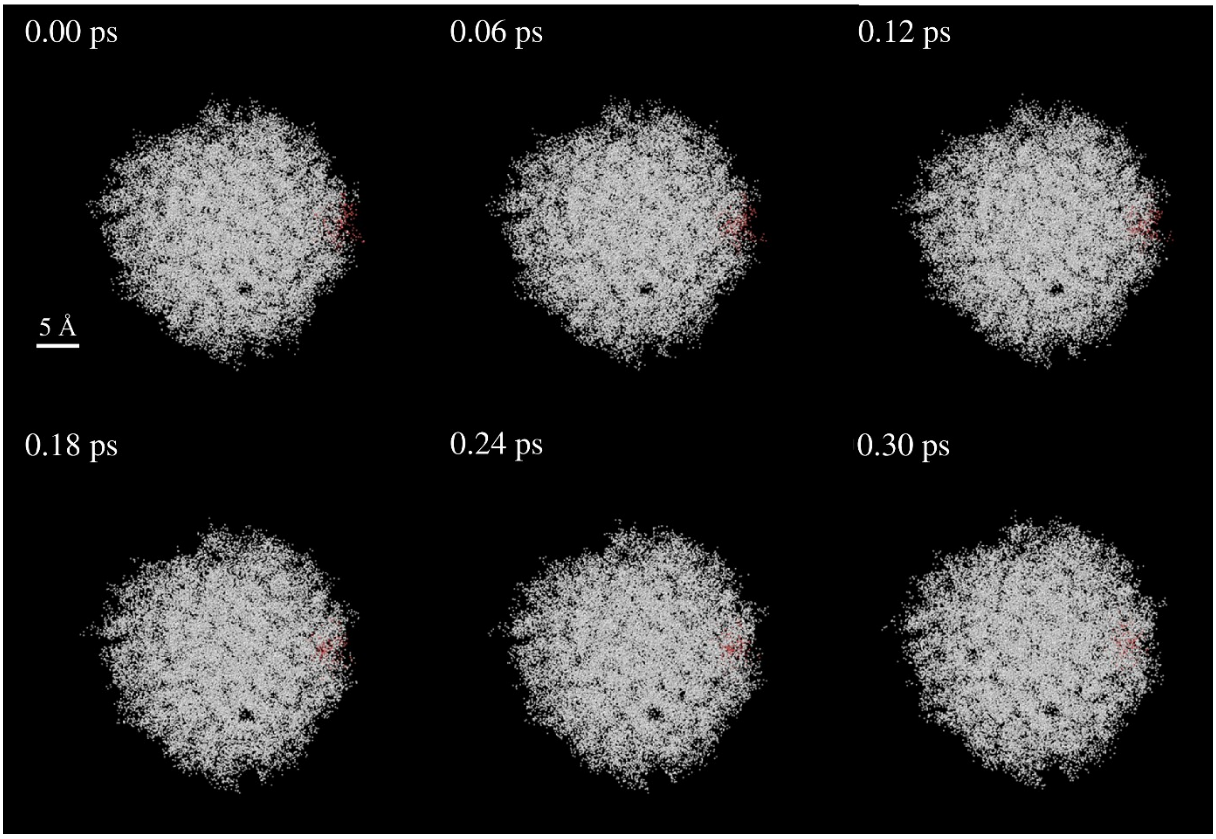

Fig. S10

Snapshots of the nonadiabatic RPMD trajectory showing dynamics evolution of the He_{300}^+ cluster when the initial ionization state is assumed to the adiabatic ground state, for which the initial charged He atom is mainly located around the surface of the cluster (a different initial structure from Fig. S8 is used). All ring-polymer beads are shown with the positively charged He atoms being shown in red color. The time interval of the snapshots is chosen to be 0.06 ps.

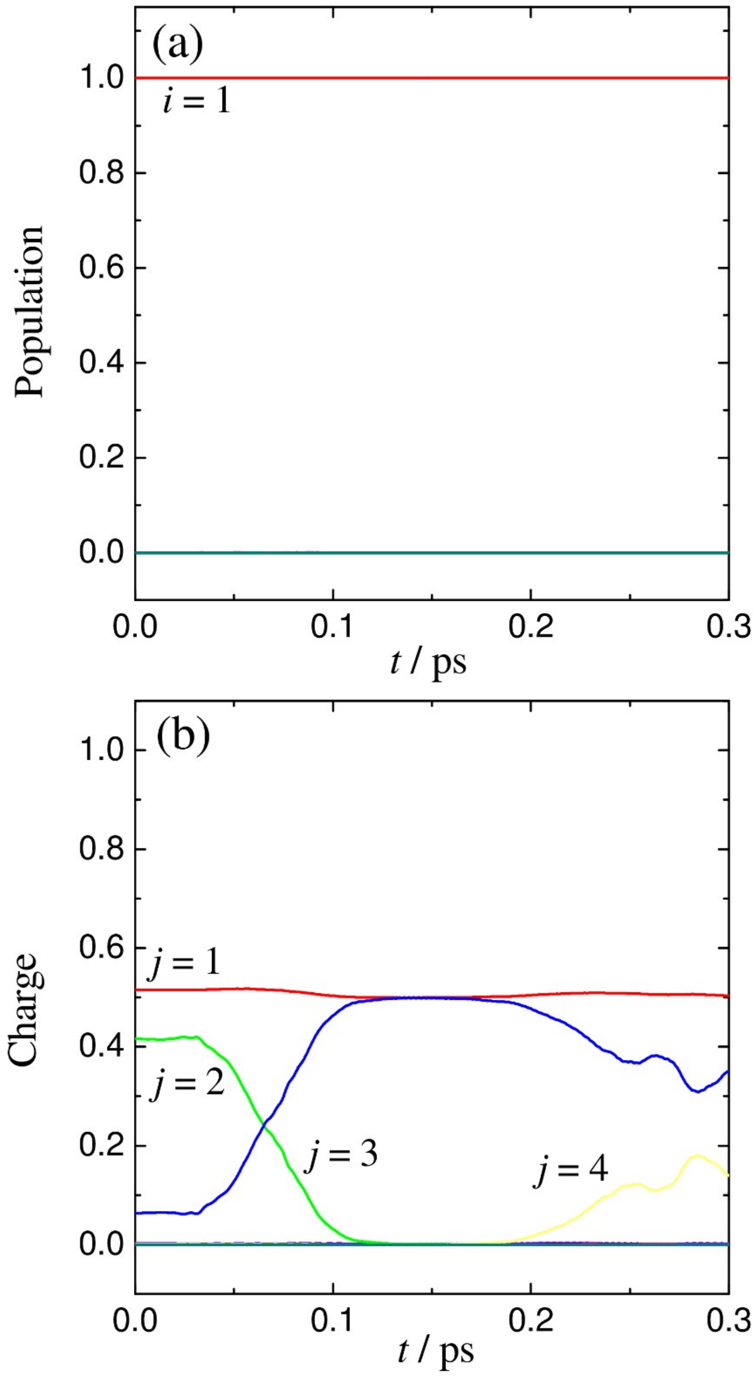

Fig. S11

Selected adiabatic populations (a) and atomic charges (b) are plotted as a function of the simulation time for the representative RPMD trajectory presented in Fig. S10.